Interaction-induced breakdown of chiral dynamics in the Su-Schrieffer-Heeger model

Yuqing Li [1,2] Yunfei Wang,[1] Hongxing Zhao,[1] Huiying Du,[1] Jiahui Zhang [1] Ying Hu,[1,2]
Feng Mei,[1,2,*] Liantuan Xiao,[1,2] Jie Ma [1,2,3,†] and Suotang Jia[1,2]

[1]*State Key Laboratory of Quantum Optics and Quantum Optics Devices, Institute of Laser Spectroscopy,*
Shanxi University, Taiyuan 030006, China
[2]*Collaborative Innovation Center of Extreme Optics, Shanxi University, Taiyuan 030006, China*
[3]*Hefei National Laboratory, Hefei 230088, China*

The effect of interparticle interactions on topological properties is difficult to experimentally probe and quantitatively characterize. For ultracold atomic systems, although topological phases and phenomena have been recently observed in various settings, the effect of atomic interactions has so far remained largely unexplored. Here, we realize a Su-Schrieffer-Heeger model in the momentum lattice of a Bose-Einstein condensate with tunable atomic interactions and measure the bulk dynamics of atoms in a synthetic topological wire subjected to sudden quench under various interactions. We observe the breakdown of chiral dynamics in the atomic wire with increasing strength of interaction, where the atoms are localized at the initial injection site under the strong interaction. We show that the mean chiral displacement can be used to characterize the effect of interaction on the atomic chiral dynamics by studying its variation with the interaction. Our results provide a benchmark for exploring the interacting topological fluids.

Introduction. Topological states of matter are a particular class of non-Landau states characterized by global topological invariants in the single-particle limit and have generated great interest in many areas of physics [1–6]. The fundamental topological phases in two dimensions are Chern insulator phases induced by breaking time-reversal symmetry that are characterized by topological Chern invariants [7,8]. The two most well-known lattice models supporting such topological phases are the Harper-Hofstadter model [9,10] and the Haldane model [11], which have been realized in ultracold atomic systems [12–15]. Moreover, several topological features, including edge states [16,17], chiral current [18–20], and quantized pumping [21,22], have been observed experimentally. In one dimension, the seminal topological phase is hosted by the paradigmatic Su-Schrieffer-Heeger (SSH) model [23], which is protected by chiral symmetry and identified by topological winding number [7,8]. The SSH model has attracted great interest for its easy implementation, as shown by experiments in optical superlattices [24] and momentum-state lattices [25]. Its chiral topological feature has been intensively explored by measuring mean chiral displacements [26–28].

Beyond noninteracting systems, investigating the effect of interaction on topological properties is of fundamental importance for understanding many exotic physical phenomena [29–31]. The interplay between topology and interactions has led to the fractional quantum Hall effect in condensed-state physics [32,33]. In photonic systems, nonlinearity, akin to interparticle interactions in the mean-field limit, has induced topological lasing [34,35], edge solitons [36,37], and quantized nonlinear Thouless pumps [38]. For ultracold atomic experiments, the highly tunable interactions offer a controllable knob to study the effect of interaction on topological properties [39]. While topology experiments in ultracold atoms have almost been restricted to the noninteracting regime, or regimes in which the weak interactions have subtle modifications, a recent experiment starts to study the impact of interaction on the topological transport [40].

Here, we experimentally realized a SSH model based on the one-dimensional (1D) momentum lattices of a Bose-Einstein condensate (BEC) of ^{133}Cs atoms with widely tunable interactions. We measure the quench dynamics of the SSH model under various interactions and study the effect of interaction on the chiral dynamics of atoms in the synthetic topological wire. The atomic chiral dynamics is broken down with increasing strength of interaction, and the atoms are localized at the initial injection site resembling a soliton state under the strong interactions. We study the variation of mean chiral displacement with the atomic interaction strength and find that it can be used to characterize the effect of interaction on the atomic chiral dynamics. Our observations show good agreement with the numerical simulations based on the Gross-Pitaevskii equation (GPE).
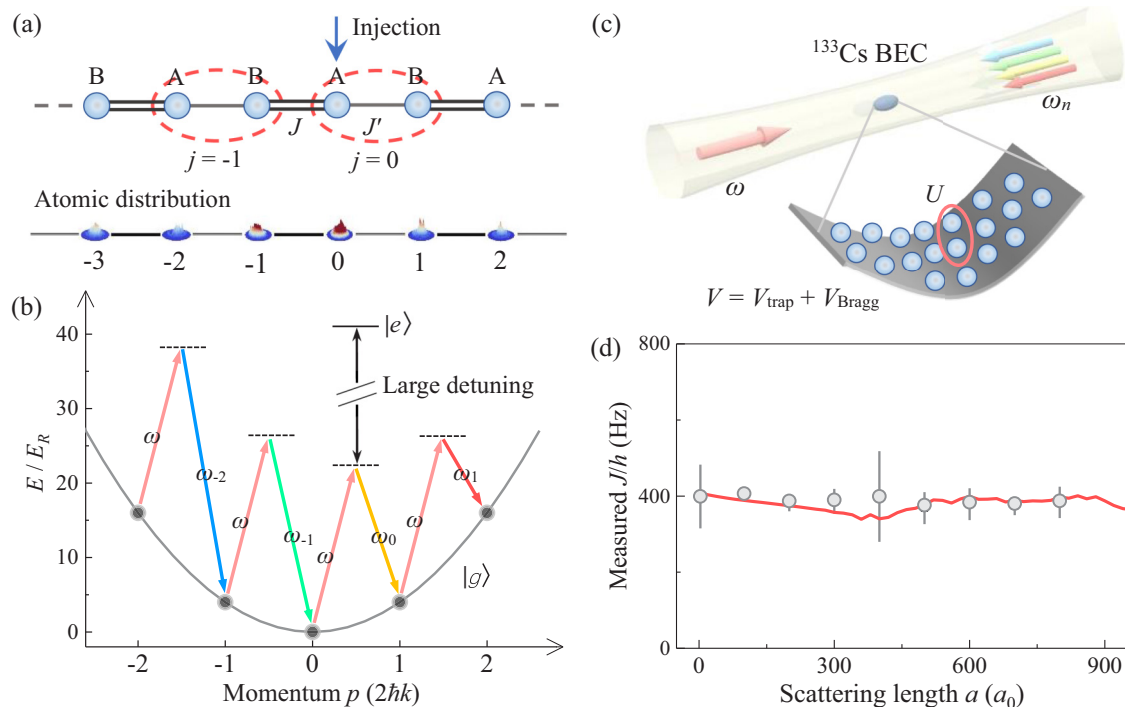
FIG. 1. Synthetic chiral topological wires based on momentum states of atoms with tunable interactions. (a) Illustration of a dimerized lattice, where the dimer cell index j ranges from -5 to 4 and the intra- and intercell tunneling energies are J' and J, respectively. At the bottom the atomic distribution in the wire can be directly obtained by the momentum-resolved absorption image. (b) A momentum lattice is used to realize the SSH model depicted in (a). A series of two-photon Bragg transitions are driven to couple the discrete atomic momentum states $p = 2n\hbar k$ ($k = 2\pi/\lambda$) with $n \in \{-10, 9\}$. The dimerized momentum lattice is synthesized by precisely controlling the strength of each Bragg transition with the alternating weak and strong forms. (c) Schematic of the experimental setup. A ^{133}Cs Bose-Einstein condensate (BEC) with tunable atomic interactions is confined in a cigar-shaped optical trap V_{trap} combined with the potential of momentum lattice V_{Bragg}, which is composed of a pair of counterpropagating laser beams, one with a single frequency ω and the other containing multiple-frequency components ω_n. The strength of atomic interaction is characterized by U. (d) Actual tunneling energy J as a function of atomic scattering length a. The solid line is the theoretical calculation based on the GPE (1). Error bars indicate fitting errors [48].

Implementation of the SSH model with tunable interactions. For atoms hopping in a dimerized lattice with two sites per unit cell in Fig. 1(a), the lattice system can be described by a SSH model, where j is the index of cell and the intra- and intercell tunneling energies are J' and J, respectively. This model supports nontrivial topological phases protected by chiral symmetry [7,23]. We implement the SSH model in a dimerized momentum lattice of a ^{133}Cs BEC with $N = 4 \times 10^4$ atoms [41–43]. A pair of counterpropagating laser beams with wavelength $\lambda = 1064$ nm are used to illuminate the atoms in a cigar-shaped trap for driving a series of two-photon Bragg transitions between discrete atomic momentum states $p = 2n\hbar k$ with the reduced Planck's constant $\hbar$ and wave vector $k = 2\pi/\lambda$ [44–47] [Figs. 1(b) and 1(c)]. Then, a dimerized lattice consisting of ten cells with $j \in \{-5, 4\}$ is synthesized by precisely controlling the strength of each Bragg transition with the unique frequency difference (see Supplemental Material [48]). The ratio of the intracell tunneling energy to the intercell tunneling energy J'/J with open boundary conditions can be tuned to prepare the system to be in different topological phases in the noninteracting regime [26,27]. Specifically, for $J'/J < 1$ the lattice system is in the nontrivial topological phase; otherwise it is in the trivial phase [48].

When introducing the interaction of atoms in the trap V_{trap} combined with the momentum lattice potential V_{Bragg} [Fig. 1(c)] by a broad Feshbach resonance [39], the time evolution of condensate wave function $\Psi(\mathbf{r}, t)$ follows the three-dimensional GPE

$$i\hbar \frac{\partial \Psi}{\partial t} = \left(-\frac{\hbar^2}{2m} \nabla^2 + V_{\mathrm{trap}} + V_{\mathrm{Bragg}} + U|\Psi|^2 \right)\Psi, \quad (1)$$

where the interaction strength is $U = 4\pi\hbar^2(N-1)a/m$ with the s-wave scattering length a, m is the atomic mass, and $\Psi(\mathbf{r}, t)$ fulfills the normalization condition of $\int |\Psi(\mathbf{r}, t)|^2 d\mathbf{r} = 1$ [49]. To avoid the significant decoherence of BEC under strong interactions, our measurement is restricted to $a \leqslant 800$ a_0 (in units of the Bohr radius). The interaction of far-detuned Bragg lasers with atoms leads to a time-dependent lattice potential $V_{\mathrm{Bragg}}(z, t) = \sum_n 2\hbar J_n \cos(2kz - \Delta\omega_n + \phi_n)$, where J_n, $\Delta\omega_n$, and $\phi_n = 0$ are the strength, detuning, and relative phase, respectively, in every Bragg transition [50,51].

To clearly illustrate the dimerized lattice form and atomic interactions in momentum lattices, we use the standard variational approach [48,49,52] to obtain the equation as the

following set:

$$i\hbar\dot{\psi}_j^A = J'\psi_j^B + J\psi_{j-1}^B + \overline{U}\big(2 - |\psi_j^A|^2\big)\psi_j^A + V\psi_j^A,$$

$$i\hbar\dot{\psi}_j^B = J'\psi_j^A + J\psi_{j+1}^A + \overline{U}\big(2 - |\psi_j^B|^2\big)\psi_j^B + V\psi_j^B, \quad (2)$$

where ψ_j^A and ψ_j^B are the wave functions of atoms at sites A and B of the jth cell. The mean-field interaction energy is given by $\overline{U} = (4\pi\hbar^2 a/m)\overline{\rho}$ with the averaged atomic density $\overline{\rho}$. As described in Refs. [53,54], the atomic interactions for $a > 0$ in the momentum lattice give rise to a density-dependent, local attractive potential, which is captured by a nonlinear term in Eq. (2), and the localization occurs when the interaction is strong enough. The additional term in Eq. (2) is $V = -\frac{\hbar^2\nabla^2}{2m} - \frac{2n\hbar k}{m}i\hbar\partial_z + V_{\text{trap}}$ with $n = 2j$ ($n = 2j + 1$) for the sublattice site A_j (B_j) in the jth cell, and the $i\partial_z$ term denotes the spatial expansion of wave function. To take into account the trap potential and the inhomogeneous atomic density in our experiment, we use the real-space GPE (1), from which Eq. (2) is derived, to perform the numerical calculation. Neglecting the trap potential V_{trap} and the inhomogeneous atomic density, Eq. (2) reduces to the nonlinear SSH model [48], and its solution shows that the population dynamics of atoms in the SSH model is reduced with increasing strength of interaction even for $\overline{U}/J < 4$. This is significantly different from self-trapping, which predicts that the diffusive dynamics of atoms in a general lattice with uniform tunneling strength is suddenly reduced at the critical interaction $\overline{U}/J = 4$ [53–56].

Prior to studying the effect of interaction on the quench dynamics of the SSH model, we measure the influence of interaction on the tunneling energy J in Fig. 1(d). The data are obtained by fitting the population dynamics of atoms at two adjacent lattice sites for various a [48]. We find that the fitted J is almost invariant within our measurement range, and this indicates that the interaction will not affect the tunneling energy, whereas its change has an impact on the tunneling dynamics.

Breakdown of chiral dynamics. The mean chiral displacement has been recently used to characterize the chiral topological features in the SSH model in the photonic system and ultracold atomic experiments in the noninteracting regime [26–28,57]. Such an observable quantity is defined as

$$C(t) = \sum_j 2j\big(P_{A_j} - P_{B_j}\big), \quad (3)$$

where P_{A_j} and P_{B_j} are the atomic populations at sites A and B of the jth cell with the normalization to the total atom number. For a nontrivial topological phase, $C(t)$ generally shows an oscillation behavior. The mean chiral displacement $\overline{C} = \lim_{T\to\infty} 1/T \int_0^T dt\, C(t)$ converges to the topological winding number and can be used to measure the Zak phase [57,58]. When the ratio is tuned from $J'/J < 1$ to $J'/J > 1$, the value of $\overline{C}$ calculated by referring to the injection site A_0 in Fig. 1(a) varies from 1 to 0 [26,27].

To study the effect of interaction on the chiral dynamics of atoms in the synthetic topological wire, we measure the dynamical evolution of atomic populations in the dimerized lattice after a sudden quench under different interactions. We initialize all atoms at site A_0 with zero momentum and then quench on the tunnel couplings with $J'/J = 0.5$ and $J/\hbar =$
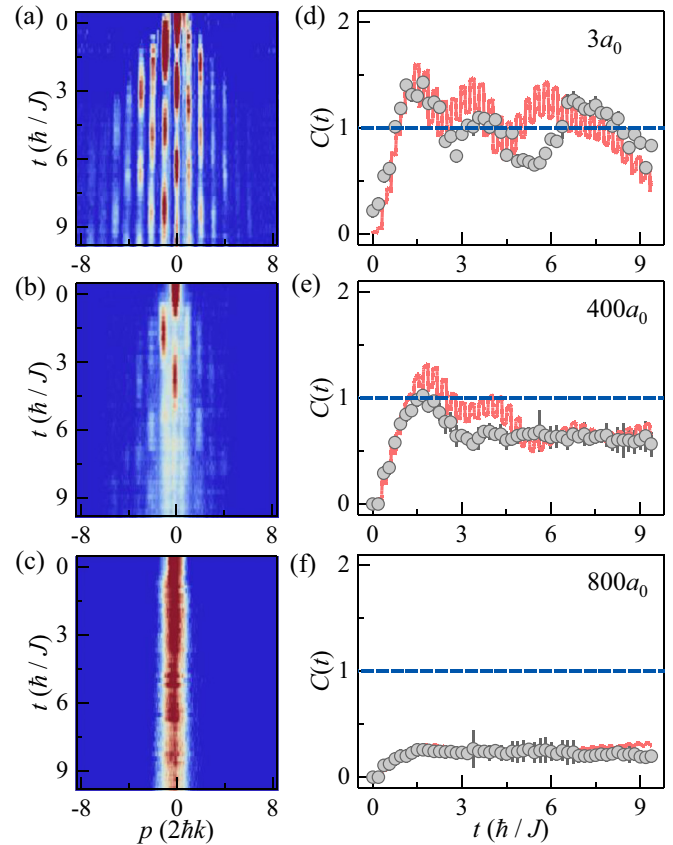
FIG. 2. Bulk dynamics and time evolution of chiral displacement under different interactions. (a)–(c) Bulk dynamics in the synthetic atomic wire are obtained by measuring the population dynamics of atoms in the dimerized lattice after a sudden quench with the tunneling energy ratio of $J'/J = 0.5$ and $J/\hbar = 2\pi \times 500$ Hz for three different scattering lengths. The momentum distribution is taken by the integrated absorption image after 22 ms time of flight. (d)–(f) Dynamical evolution of chiral displacement $C(t)$ extracted from the data in (a)–(c), respectively. The solid red curves are the numerical simulations based on the GPE (1). All error bars denote standard errors.

$2\pi \times 500$ Hz. The subsequent dynamics in Figs. 2(a)–2(c) for three different interactions are obtained by taking a series of absorption images after the variable evolution time t (in units of the tunneling time $\hbar/J \approx 320$ μs) and 22 ms time of-flight. In the noninteracting regime with $a = 3\, a_0$, the population dynamics of atoms is supported by the alternating weak and strong hoppings, since the initial state is projected on the eigenstate of the quenched lattice system. For $a = 400\, a_0$, the atomic diffusion is reduced significantly. For $a = 800\, a_0$, the atoms become localized at the initial injection site. The blurred boundary between the adjacent sites in Figs. 2(b) and 2(c) is likely caused by the broadening of the atomic width at lattice sites under the strong interaction. We also show the effect of interaction on the atomic chiral dynamics for two different dimerizations, $J'/J = 0.25$ and 0.75, in the Supplemental Material [48].

From the data in Figs. 2(a)–2(c), we extract the evolution of $C(t)$ in Figs. 2(d)–2(f) according to Eq. (3). For $a = 3\, a_0$, the strong dimerization produces a large energy gap in the
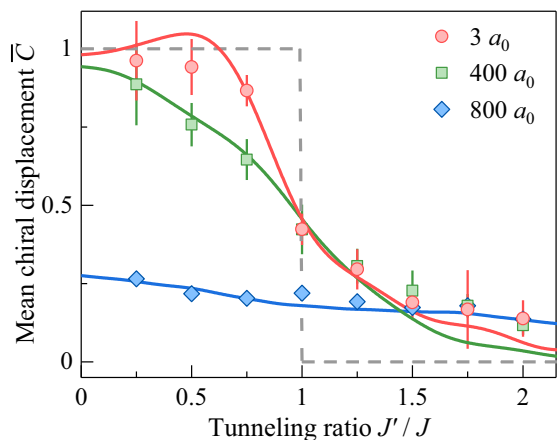
FIG. 3. Effect of interaction on the variation of mean chiral displacement with the tunneling energy ratio J'/J. The mean chiral displacement $\overline{C}$ as a function of J'/J is shown for three different scattering lengths. Each $\overline{C}$ is obtained by the time-averaged $C(t)$ in the time range from $4\,\hbar/J$ to $9.4\,\hbar/J$. Solid lines are the numerical simulations based on the GPE (1), and the gray dashed line is the prediction from a tight-binding model in the noninteracting limit. All error bars denote the standard deviations of the mean. The intercell tunneling energies are fixed at $J/\hbar = 2\pi \times 500$ Hz.

FIG. 4. Effect of interaction on the mean chiral displacement for three different tunneling energy ratios. The mean chiral displacement $\overline{C}$ is shown as a function of scattering length a for $J'/J = 0.25$, 0.5, and 0.75 with $J/\hbar = 2\pi \times 500$ Hz. For each a, $\overline{C}$ is obtained by averaging the dynamical $C(t)$ in time over the range from $4\,\hbar/J$ to $9.4\,\hbar/J$. The mean-field energy $\overline{U}/J$ is calculated with the averaged atomic density. The solid line represents the numerical simulation of the GPE (1). The error bars denote the standard deviations of the mean.

band structure in a topological phase; $C(t)$ exhibits a damping oscillation, and the mean chiral displacement $\overline{C}$ converges to 1. The atomic chiral dynamics is broken down with increasing strength of interaction, where $\overline{C}$ is slightly below 1 for $a = 400\,a_0$ and $\overline{C} \ll 1$ for $a = 800\,a_0$. These data qualitatively agree with the numerical simulation based on the GPE (1). Compared with the noninteracting case, the reduction in chiral dynamics at $a = 400\,a_0$ can be reflected by the value of the mean chiral displacement with $\overline{C} < 1$.

Effect of interaction on mean chiral displacement. Based on the dynamics of $C(t)$ under various interactions, we study the effect of interaction on the variation of mean chiral displacement $\overline{C}$ with the ratio J'/J for $J/\hbar = 2\pi \times 500$ Hz in Fig. 3. $\overline{C}$ is determined by averaging $C(t)$ in time over the range from $4\,\hbar/J$ to $9.4\,\hbar/J$ [26,48]. In the noninteracting regime, we observe a phase transition from topological ($\overline{C} = 1$) to trivial ($\overline{C} = 0$) when the ratio is tuned from $J'/J < 1$ to $J'/J > 1$, as shown in previous experiments [26–28]. Different from the ideal case (dashed line), the observed transition exhibits a smooth crossover with finite evolution time ($t \sim 9.4\,\hbar/J$) and small lattice size.

However, for $a = 400\,a_0$, $\overline{C}$ begins to drop below 1 at low J'/J, and the values of $\overline{C}$ are significantly smaller than the noninteracting cases for $J'/J < 1$. When the interaction is increased to $a = 800\,a_0$, we find $\overline{C} < 0.5$ even for $J'/J \ll 1$, and the topological phase transition induced by the change in J'/J collapses. This is mainly attributed to the breakdown of chiral dynamics in the atomic wire under the strong interaction. Our experimental data agree well with the numerical simulations based on the GPE (1).

We further study the dependence of $\overline{C}$ on the interaction for three different J'/J in Fig. 4. The value of $\overline{C}$ is close to 1 in the range $\overline{U}/J \leqslant 1$, but $\overline{C}$ starts to decrease with increasing strength of interaction for $\overline{U}/J > 1$. For the atoms

in the nonlinear SSH model, the momentum width starts to decrease at the weaker interaction [48] compared with $\overline{C}$, where the momentum width has been used to characterize the localization degree in a study of self-trapping in momentum lattices [54]. Thus $\overline{C}$ can be used to characterize the effect of interaction on the atomic chiral dynamics in the SSH model rather than the self-trapping. Compared with the nonlinear SSH model that predicts a large reduction in $\overline{C}$ at $\overline{U}/J = 4$ [48], the experimental data are in good agreement with the numerical simulations based on the GPE (1), where the influence of trap potential and inhomogeneous atomic density in the experiment is accurately taken into account.

In addition, considering the widely tunable range for the interactions of ^{133}Cs atoms, we show the influence of the attractive interaction on $\overline{C}$ by measuring the dynamics of the SSH model for $a < 0$ [48]. Both the data and theoretical calculation show that $\overline{C}$ begins to decrease under the weakly attractive interactions. The discrepancy between the experiment and theory is likely caused by the excitation of condensate in Feshbach tuning to $a < 0$ [39], which generates thermal atoms and then reduces the coupling efficiency in Bragg transitions.

Conclusion. We have performed an experimental study of the effect of interaction on the dynamics of the SSH model by tuning atomic interactions and tunneling energies in a dimerized momentum lattice. Based on the population dynamics of atoms under different interactions, we have found the breakdown of atomic chiral dynamics with increasing strength of interaction. We also show that the mean chiral displacement allows us to characterize the effect of interaction on the chiral dynamics in a synthetic atomic wire. Our study paves the way for understanding the effect of interaction on

topological phases and further exploring many exotic physical phenomena.

[1] M. Z. Hasan and C. L. Kane, Colloquium: Topological insulators, Rev. Mod. Phys. **82**, 3045 (2010).

[2] X.-L. Qi and S.-C. Zhang, Topological insulators and superconductors, Rev. Mod. Phys. **83**, 1057 (2011).

[3] L. Lu, J. D. Joannopoulos, and M. Soljačić, Topological photonics, Nat. Photonics **8**, 821 (2014).

[4] S. D. Huber, Topological mechanics, Nat. Phys. **12**, 621 (2016).

[5] N. Goldman, J. C. Budich, and P. Zoller, Topological quantum matter with ultracold gases in optical lattices, Nat. Phys. **12**, 639 (2016).

[6] N. R. Cooper, J. Dalibard, and I. B. Spielman, Topological bands for ultracold atoms, Rev. Mod. Phys. **91**, 015005 (2019).

[7] S. Ryu, A. P. Schnyder, A. Furusaki, and A. W. W. Ludwig, Topological insulators and superconductors: tenfold way and dimensional hierarchy, New J. Phys. **12**, 065010 (2010).

[8] C.-K. Chiu, J. C. Y. Teo, A. P. Schnyder, and S. Ryu, Classification of topological quantum matter with symmetries, Rev. Mod. Phys. **88**, 035005 (2016).

[9] P. G. Harper, Single band motion of conduction electrons in a uniform magnetic field, Proc. Phys. Soc. A **68**, 874 (1955).

[10] D. R. Hofstadter, Energy levels and wave functions of Bloch electrons in rational and irrational magnetic fields, Phys. Rev. B **14**, 2239 (1976).

[11] F. D. M. Haldane, Model for a Quantum Hall Effect without Landau Levels: Condensed-Matter Realization of the "Parity Anomaly", Phys. Rev. Lett. **61**, 2015 (1988).

[12] M. Aidelsburger, M. Atala, M. Lohse, J. T. Barreiro, B. Paredes, and I. Bloch, Realization of the Hofstadter Hamiltonian with Ultracold Atoms in Optical Lattices, Phys. Rev. Lett. **111**, 185301 (2013).

[13] H. Miyake, G. A. Siviloglou, C. J. Kennedy, W. C. Burton, and W. Ketterle, Realizing the Harper Hamiltonian with Laser-Assisted Tunneling in Optical Lattices, Phys. Rev. Lett. **111**, 185302 (2013).

[14] M. Aidelsburger, M. Lohse, C. Schweizer, M. Atala, J. T. Barreiro, S. Nascimbène, N. R. Cooper, I. Bloch, and N. Goldman, Measuring the Chern number of Hofstadter bands with ultracold bosonic atoms, Nat. Phys. **11**, 162 (2015).

[15] G. Jotzu, M. Messer, R. Desbuquois, M. Lebrat, T. Uehlinger, D. Greif, and T. Esslinger, Experimental realization of the topological Haldane model with ultracold fermions, Nature (London) **515**, 237 (2014).

[16] M. Mancini, G. Pagano, G. Cappellini, L. Livi, M. Rider, J. Catani, C. Sias, P. Zoller, M. Inguscio, M. Dalmonte, and L. Fallani, Observation of chiral edge states with neutral fermions in synthetic Hall ribbons, Science **349**, 1510 (2015).

[17] B. K. Stuhl, H.-I. Lu, L. M. Aycock, D. Genkina, and I. B. Spielman, Visualizing edge states with an atomic Bose gas in the quantum Hall regime, Science **349**, 1514 (2015).

[18] M. Atala, M. Aidelsburger, M. Lohse, J. T. Barreiro, B. Paredes, and I. Bloch, Observation of chiral currents with ultracold atoms in bosonic ladders, Nat. Phys. **10**, 588 (2014).

[19] S. Kolkowitz, S. L. Bromley, T. Bothwell, M. L. Wall, G. E. Marti, A. P. Koller, X. Zhang, A. M. Rey, and J. Ye, Spin-orbit-coupled fermions in an optical lattice clock, Nature (London) **542**, 66 (2017).

[20] F. A. An, E. J. Meier, and B. Gadway, Direct observation of chiral currents and magnetic reflection in atomic flux lattices, Sci. Adv. **3**, e1602685 (2017).

[21] S. Nakajima, T. Tomita, S. Taie, T. Ichinose, H. Ozawa, L. Wang, M. Troyer, and Y. Takahashi, Topological Thouless pumping of ultracold fermions, Nat. Phys. **12**, 296 (2016).

[22] M. Lohse, C. Schweizer, O. Zilberberg, M. Aidelsburger, and I. Bloch, A Thouless quantum pump with ultracold bosonic atoms in an optical superlattice, Nat. Phys. **12**, 350 (2016).

[23] W. P. Su, J. R. Schrieffer, and A. J. Heeger, Solitons in Polyacetylene, Phys. Rev. Lett. **42**, 1698 (1979).

[24] M. Atala, M. Aidelsburger, J. T. Barreiro, D. Abanin, T. Kitagawa, E. Demler, and I. Bloch, Direct measurement of the Zak phase in topological Bloch bands, Nat. Phys. **9**, 795 (2013).

[25] E. J. Meier, F. A. An, and B. Gadway, Observation of the topological soliton state in the Su-Schrieffer-Heeger model, Nat. Commun. **7**, 13986 (2016).

[26] E. J. Meier, F. A. An, A. Dauphin, M. Maffei, P. Massignan, T. L. Hughes, and B. Gadway, Observation of the topological Anderson insulator in disordered atomic wires, Science **362**, 929 (2018).

[27] D. Z. Xie, W. Gou, T. Xiao, B. Gadway, and B. Yan, Topological characterizations of an extended Su-Schrieffer-Heeger model, npj Quantum Inf. **5**, 55 (2019).

[28] D. Z. Xie, T.-S. Deng, T. Xiao, W. Gou, T. Chen, W. Yi, and B. Yan, Topological Quantum Walks in Momentum Space with a Bose-Einstein Condensate, Phys. Rev. Lett. **124**, 050502 (2020).

[29] J. Maciejko and G. A. Fiete, Fractionalized topological insulators, Nat. Phys. **11**, 385 (2015).

[30] S. Rachel, Interacting topological insulators: A review, Rep. Prog. Phys. **81**, 116501 (2018).

[31] D.-W. Zhang, Y.-Q. Zhu, Y. X. Zhao, H. Yan, and S.-L. Zhu, Topological quantum matter with cold atoms, Adv. Phys. **67**, 253 (2018).

[32] D. C. Tsui, H. L. Stormer, and A. C. Gossard, Two-Dimensional Magnetotransport in the Extreme Quantum Limit, Phys. Rev. Lett. **48**, 1559 (1982).

[33] R. B. Laughlin, Anomalous Quantum Hall Effect: An Incompressible Quantum Fluid with Fractionally Charged Excitations, Phys. Rev. Lett. **50**, 1395 (1983).

[34] P. St-Jean, V. Goblot, E. Galopin, A. Lemaître, T. Ozawa, L. Le Gratiet, I. Sagnes, J. Bloch, and A. Amo, Lasing in topological

edge states of a one-dimensional lattice, Nat. Photonics **11**, 651 (2017).

[35] M. A. Bandres, S. Wittek, G. Harari, M. Parto, J. Ren, M. Segev, D. N. Christodoulides, and M. Khajavikhan, Topological insulator laser: Experiments, Science **359**, eaar4005 (2018).

[36] S. Mukherjee and M. C. Rechtsman, Observation of Unidirectional Solitonlike Edge States in Nonlinear Floquet Topological Insulators, Phys. Rev. X **11**, 041057 (2021).

[37] Y. V. Kartashov, A. A. Arkhipova, S. A. Zhuravitskii, N. N. Skryabin, I. V. Dyakonov, A. A. Kalinkin, S. P. Kulik, V. O. Kompanets, S. V. Chekalin, L. Torner, and V. N. Zadkov, Observation of Edge Solitons in Topological Trimer Arrays, Phys. Rev. Lett. **128**, 093901 (2022).

[38] M. Jürgensen, S. Mukherjee, and M. C. Rechtsman, Quantized nonlinear Thouless pumping, Nature (London) **596**, 63 (2021).

[39] C. Chin, R. Grimm, P. Julienne, and E. Tiesinga, Feshbach resonances in ultracold gases, Rev. Mod. Phys. **82**, 1225 (2010).

[40] A.-S. Walter, Z. J. Zhu, M. Gächter, J. Minguzzi, S. Roschinski, K. Sandholzer, K. Viebahn, and T. Esslinger, Quantization and its breakdown in a Hubbard–Thouless pump, Nat. Phys. (2023), doi:10.1038/s41567-023-02145-w.

[41] T. Weber, J. Herbig, M. Mark, H.-C. Nägerl, and R. Grimm, Bose-Einstein condensation of cesium, Science **299**, 232 (2003).

[42] T. Kraemer, J. Herbig, M. Mark, T. Weber, C. Chin, H.-C. Nägerl, and R. Grimm, Optimized production of a cesium Bose-Einstein condensate, Appl. Phys. B **79**, 1013 (2004).

[43] Y. F. Wang, Y. Q. Li, J. Z. Wu, W. L. Liu, J. Z. Hu, J. Ma, L. T. Xiao, and S. T. Jia, Hybrid evaporative cooling of ^{133}Cs atoms to Bose-Einstein condensation, Opt. Express **29**, 13960 (2021).

[44] E. J. Meier, F. A. An, and B. Gadway, Atom-optics simulator of lattice transport phenomena, Phys. Rev. A **93**, 051602(R) (2016).

[45] F. A. An, E. J. Meier, and B. Gadway, Diffusive and arrested transport of atoms under tailored disorder, Nat. Commun. **8**, 325 (2017).

[46] Y. Q. Li, J. H. Zhang, Y. F. Wang, H. Y. Du, J. Z. Wu, W. L. Liu, F. Mei, J. Ma, L. T. Xiao, and S. T. Jia, Atom-optically synthetic gauge fields for a noninteracting Bose gas, Light Sci. Appl. **11**, 13 (2022).

[47] Y. F. Wang, J.-H. Zhang, Y. Q. Li, J. Z. Wu, W. L. Liu, F. Mei, Y. Hu, L. T. Xiao, J. Ma, C. Chin, and S. T. Jia, Observation of Interaction-Induced Mobility Edge in an Atomic Aubry-André Wire, Phys. Rev. Lett. **129**, 103401 (2022).

[48] See Supplemental Material at http://link.aps.org/supplemental/10.1103/PhysRevResearch.5.L032035 for details of our experiments, the single-particle topological edge states, the actual tunneling energies, the measurement of atomic population dynamics, the effect of interaction on the chiral dynamics for different dimerizations, the interaction of Bragg laser fields with atoms, the derivation of the Hamiltonian in a dimerized lattice, the real-space GPE simulation, the nonlinear SSH model, a comparison of the interaction effect on chiral dynamics with self-trapping, and the chiral dynamics under attractive interactions.

[49] C. J. Pethick and H. Smith, *Bose-Einstein Condensation in Dilute Gases* (Cambridge University Press, Cambridge, 2008).

[50] P. B. Blakie and R. J. Ballagh, Mean-field treatment of Bragg scattering from a Bose-Einstein condensate, J. Phys. B: At. Mol. Opt. Phys. **33**, 3961 (2000).

[51] S. Pötting, M. Cramer, and P. Meystre, Momentum-state engineering and control in Bose-Einstein condensates, Phys. Rev. A **64**, 063613 (2001).

[52] T. Chen, D. Z. Xie, B. Gadway, and B. Yan, A Gross-Pitaevskii-equation description of the momentum-state lattice: Roles of the trap and many-body interactions, arXiv:2103.14205 v2.

[53] F. A. An, E. J. Meier, J. Ang'ong'a, and B. Gadway, Correlated Dynamics in a Synthetic Lattice of Momentum States, Phys. Rev. Lett. **120**, 040407 (2018).

[54] F. A. An, B. Sundar, J. P. Hou, X.-W. Luo, E. J. Meier, C. W. Zhang, K. R. A. Hazzard, and B. Gadway, Nonlinear Dynamics in a Synthetic Momentum-State Lattice, Phys. Rev. Lett. **127**, 130401 (2021).

[55] S. Raghavan, A. Smerzi, S. Fantoni, and S. R. Shenoy, Coherent oscillations between two weakly coupled Bose-Einstein condensates: Josephson effects, π oscillations, and macroscopic quantum self-trapping, Phys. Rev. A **59**, 620 (1999).

[56] M. Albiez, R. Gati, J. Fölling, S. Hunsmann, M. Cristiani, and M. K. Oberthaler, Direct Observation of Tunneling and Nonlinear Self-Trapping in a Single Bosonic Josephson Junction, Phys. Rev. Lett. **95**, 010402 (2005).

[57] F. Cardano, A. D'Errico, A. Dauphin, M. Maffei, B. Piccirillo, C. D. Lisio, G. D. Filippis, V. Cataudella, E. Santamato, L. Marrucci, M. Lewenstein, and P. Massignan, Detection of Zak phases and topological invariants in a chiral quantum walk of twisted photons, Nat. Commun. **8**, 15516 (2017).

[58] Z.-Q. Jiao, S. Longhi, X.-W. Wang, J. Gao, W.-H. Zhou, Y. Wang, Y.-X. Fu, L. Wang, R.-J. Ren, L.-F. Qiao, and X.-M Jin, Experimentally Detecting Quantized Zak Phases without Chiral Symmetry in Photonic Lattices, Phys. Rev. Lett. **127**, 147401 (2021).